HHS Public Access

Author manuscript

Dev Biol. Author manuscript; available in PMC 2020 February 18.

Published in final edited form as:

Dev Biol. 2016 March 15; 411(2): 266–276. doi:10.1016/j.ydbio.2015.12.016.

BMPs are direct triggers of interdigital programmed cell death

Maria M. Kaltcheva[a], **Matthew J. Anderson**[a], **Brian D. Harfe**[b], **Mark Lewandoski**[a,*]

[a]Genetics of Vertebrate Development Section, Cancer and Developmental Biology Lab, National Cancer Institute, National Institutes of Health, Frederick, MD21702, USA

[b]Department of Molecular Genetics and Microbiology, The Genetics Institute, University of Florida, Gainesville, FL 32610, USA

Abstract

During vertebrate embryogenesis the interdigital mesenchyme is removed by programmed cell death (PCD), except in species with webbed limbs. Although bone morphogenetic proteins (BMPs) have long been known to be players in this process, it is unclear if they play a direct role in the interdigital mesenchyme or if they only act indirectly, by affecting fibroblast growth factor (FGF) signaling. A series of genetic studies have shown that BMPs act indirectly by regulating the withdrawal of FGF activity from the apical ectodermal ridge (AER); this FGF activity acts as a cell survival factor for the underlying mesenchyme. Other studies using exogenous factors to inhibit BMP activity in explanted mouse limbs suggest that BMPs do not act directly in the mesenchyme. To address the question of whether BMPs act directly, we used an interdigit-specific Cre line to inactivate several genes that encode components of the BMP signaling pathway, without perturbing the normal downregulation of AER-FGF activity. Of three *Bmps* expressed in the interdigital mesenchyme, *Bmp7* is necessary for PCD, but *Bmp2* and *Bmp4* both have redundant roles, with *Bmp2* being the more prominent player. Removing BMP signals to the interdigit by deleting the receptor gene, *Bmpr1a*, causes a loss of PCD and syndactyly, thereby unequivocally proving that BMPs are direct triggers of PCD in this tissue. We present a model in which two events must occur for normal interdigital PCD: the presence of a BMP death trigger and the absence of an FGF survival activity. We demonstrate that neither event is required for formation of the interdigital vasculature, which is necessary for PCD. However, both events converge on the production of reactive oxygen species that activate PCD.

Keywords

BMP; FGF; Limb development; Programmed cell death; Reactive oxygen species; Syndactyly

1. Introduction

Programmed cell death (PCD) is an evolutionarily conserved and genetically regulated mechanism necessary for normal embryogenesis (Conradt, 2009; Zakeri et al., 2015). In

*Corresponding author. Lewandom@mail.nih.gov (M. Lewandoski).

Appendix A. Supplementary material

Supplementary data associated with this article can be found in the online version at http://dx.doi.org/10.1016/j.ydbio.2015.12.016.

mammals, PCD is essential for various aspects of development, including retinal development in the eye (Braunger et al., 2014; Elliott et al., 2006; Young, 1984), neuronal trimming during development of the central nervous system (Lossi and Gambino, 2008), sex differentiation (Dyche,1979; Teixeira et al., 2001), and development of the immune system (Takeuchi et al., 2005). Furthermore, misregulation of cell death, either through the reduction or enhancement of PCD, results in many diseases such as cancer, Alzheimer's, and multiple sclerosis (Hassan et al., 2014; Tower, 2015; Vermeulen et al., 2005). Therefore, a better understanding of the pathways involved in PCD regulation would provide insight into normal development as well as what goes awry in these pathogenic states.

One well-characterized model of PCD during embryogenesis is the developing limb, in which cell death is necessary to remove interdigit (ID) tissue to allow proper separation of the digits (Hernandez-Martinez and Covarrubias, 2011; Lorda-Diez et al., 2015; Montero and Hurle, 2010). The three main signaling pathways that control interdigital PCD are those governed by retinoic acid (RA), fibroblast growth factors (FGFs), and bone morphogenetic proteins (BMPs) (Hernandez-Martinez and Covarrubias, 2011). RA is thought to induce interdigital PCD because application of RA accelerates the process of ID regression (Hernandez-Martinez et al., 2009; Lussier et al., 1993; Rodriguez-Leon et al., 1999) whereas an RA antagonist, AGN193109, inhibits it (Hernandez-Martinez et al., 2009; Rodriguez-Leon et al., 1999). Furthermore, syndactyly, or webbing between the digits due to a failure of interdigital tissue elimination, occurs in mouse mutants with compound somatic inactivations of *Rar* (Ghyselinck et al., 1997) and *Rxr* (Kastner et al., 1997), which encode receptors necessary for RA signaling, as well as *Raldh2* mutants, which lack the main aldehyde dehydrogenase responsible for RA synthesis (Zhao et al., 2010). On the other hand, FGFs act as cell survival factors that have been shown to interact antagonistically with RA in the regulation of interdigital PCD (Hernandez-Martinez et al., 2009; Hernandez-Martinez and Covarrubias, 2011). FGF8 is secreted from the apical ectodermal ridge (AER), a structure located at the dorso-ventral boundary of the distal limb. The timing of AER-*Fgf8* downregulation overlying the interdigital mesenchyme closely correlates with PCD initiation and progression (Salas-Vidal et al., 2001). In support of FGFs' cell survival role, FGF2-, FGF4-, or FGF8-soaked beads inhibit interdigital PCD in chick (Macias et al., 1996) and mouse (Hernandez-Martinez et al., 2009; Ngo-Muller and Muneoka, 2000) and transgenic overexpression of *Fgf4* in the AER leads to syndactyly through a loss of interdigital PCD (Lu et al., 2006). In addition, inhibiting FGF receptors in mouse limb cultures increases mesenchymal cell death (Hernandez-Martinez et al., 2009), whereas humans harboring mutations that cause constitutively active FGF receptors, in Apert or Pfeiffer syndromes, present with webbing of the hands and feet (Wilkie et al., 2002).

The exact role of BMP signaling in interdigital PCD is uncertain. Earlier models proposed that BMPs were direct cell death triggers signaling to the interdigital mesenchyme (Zuzarte-Luis and Hurle, 2002, 2005). In 2007 we demonstrated an indirect role by inactivating the BMP receptor gene, *Bmpr1a*, specifically in the mouse AER, and showed that BMP signals were required to downregulate AER-FGF cell-survival activity over the ID (Pajni-Underwood et al., 2007). Evidence that the BMP-SMAD pathway was essential for this indirect BMP role in PCD has since been found in mouse AER-specific inactivations of *Bmp2* and *Bmp4*, (Choi et al., 2012; Maatouk et al., 2009), *Smad1/Smad5* (Wong et al.,

2012), and *Smad4* (Benazet and Zeller, 2013), all of which result in prolonged AER-FGF signals and syndactyly.

Compared to these genetic data, the evidence for a direct BMP death signal is somewhat ambiguous. *Bmp2, Bmp4,* and *Bmp7* are expressed throughout the interdigital mesenchyme during mouse and chick limb development (Pajni-Underwood et al., 2007; Robert, 2007; Salas-Vidal et al., 2001). In chick, application of BMP-coated beads in the interdigital mesenchyme increases cell death and accelerates regression of the ID (Macias et al., 1997; Yokouchi et al., 1996; Zuzarte-Luis et al., 2004). Conversely, avian interdigital PCD is inhibited when BMP signaling is blocked by inserting GREMLIN-coated beads (Merino et al., 1999) or infecting with a retroviral vector expressing a dominant negative BMP receptor (Yokouchi et al., 1996; Zou and Niswander, 1996). None of these studies explored whether these manipulations affected AER-FGF activity, which, if altered, would confound a straightforward interpretation of the data. Indeed, Hernández-Martínez et al. found that a NOGGIN-soaked bead in the chick interdigital mesenchyme can prolong AER-FGF activity, depending on where it is placed proximal-distally (Hernandez-Martinez et al., 2009). Mouse studies purporting to demonstrate a direct role for BMPs in PCD involve overexpression of the BMP antagonist gene, *Noggin,* in the AER (Guha et al., 2002; Wang et al., 2004) or inactivation of *Bmp2* and *Bmp4* specifically in the limb bud mesenchyme (Bandyopadhyay et al., 2006). In these studies both syndactyly and an upregulation of AER-*Fgf8* occurred, obscuring the meaning of the phenotype. Furthermore, Covarrubias and coworkers have argued that the timing and domains of *Bmp2, Bmp4,* or *Bmp7* expression in the mouse ID does not coincide with PCD in this tissue (Hernandez-Martinez and Covarrubias, 2011; Salas-Vidal et al., 2001). Also, they found that a NOGGIN-soaked bead inserted into the mouse ID or treatment with the SMAD-inhibitor, dorsomorphin, has no effect on PCD. Therefore they proposed that in the mouse BMPs do not have a direct role in interdigital PCD (Hernandez-Martinez et al., 2009). However, in the absence of a direct genetic test that diminishes BMP signals to the ID without affecting AER-*Fgf* expression, it is not clear what is the exact role of BMP signaling in interdigital PCD.

Here we describe such genetic studies, in which we inactivate specific genes of the BMP signaling pathway and conclusively demonstrate a direct role for BMP signaling in interdigital PCD. We then compare these mutants with our previously described mouse model whereby syndactyly occurs because of prolonged AER-FGF signaling (Pajni-Underwood et al., 2007) and examine interdigital vascular formation and reactive oxygen species (ROS) production, both recently shown to be needed for normal PCD (Eshkar-Oren et al., 2015). We found that the interdigital vasculature is unaffected in either mutant, however ROS production is markedly reduced in the absence of BMP signaling or prolonged presence of an FGF signal. Therefore, we propose a “two event model” whereby normal ROS-mediated interdigital cell death requires a direct BMP cell death signal and the removal of an FGF cell survival signal. The absence of either event results in syndactyly.

2. Materials and methods

2.1. Generation of mice and embryos

Mice were maintained on a mixed (NIH/Swiss/129SvEv/C57BL/6) background. Mutant and control mice/embryos were produced using the mating strategy described in Table 1, with the females listed first in the experimental cross. Mice carrying Msx2Cre closely linked to *Bmpr1a*^{null} are previously described (Pajni-Underwood et al., 2007). Genotyping and PCR conditions have been previously described for the following alleles: Osr1Cre (Grieshammer et al., 2008), *Bmp2*^{flox} (Ma and Martin, 2005), *Bmp4*^{flox} and *Bmp4*^{null} (Chang et al., 2008), *Bmp7*^{flox} (Zouvelou et al., 2009), *Bmpr1a*^{flox} (Mishina et al., 2002), *Bmpr1a*^{null} (Mishina et al., 2002), *Rosa26*^{R26R} (Soriano, 1999), and *Rosa26*^{mTmG} (Muzumdar et al., 2007). In Figs. 4 and 5 parents were also heterozygous for *Bmpr1b*^{null}. Note, because forelimb development is approximately 10–12 hours ahead of hindlimb development, in Figs. 5 and 6, to obtain appropriately stage-matched limbs, Msx2Cre; *Bmpr1a*$^{flox/null}$ forelimbs were harvested approximately 10 hours prior to Osr1Cre; *Bmpr1a*$^{flox/null}$ hindlimbs.

2.2. Whole-mount in situ hydridization, LysoTracker Red, reactive oxygen species, and β-galactosidase assays

mRNA whole-mount in *situ* hybridization (WISH) (Naiche et al., 2011), cell death detection via LysoTracker Red (Molecular Probes L-7528) (Grieshammer et al., 2005), reactive oxygen species detection via Dihydroethidium (Life Technologies D-1168) (Eshkar-Oren et al., 2015), and β-galactosidase staining (Anderson et al., 2013) were performed as previously described. In all WISH assays, experimental embryos and the corresponding littermate controls were processed in the same tube throughout the procedure. For AER-*Fgf8* WISH assays minimal proteinase-K incubations were performed.

2.3. Whole-mount immunolabeling

Colorimetric (Joyner and Wall, 2008) and fluorescent (Eshkar-Oren et al., 2015) whole-mount immunolabeling was performed as previously described. Cleaved Caspase-3 (Asp175) (CST #9661) was used at a concentration of 1:100 and visualized using DAB/NiCl (Joyner and Wall, 2008). Vascular patterning was detected using PECAM-1 (CD31) (Pharmingen PMG550274) at a concentration of 1:25 (Eshkar-Oren et al., 2015). For PECAM-1 immunofluorescence, a biotin-SP-conjugated AffiniPure donkey anti-rat IG (Jackson Lab. 712–065–153) was used at 1:100 dilution, followed by a one hour room temperature incubation with Alexa fluor 488-streptavidin (Jackson Lab. 016–540–084) at a 1:100 dilution. pSMAD 1, 5 immunofluorescence was detected using a primary antibody from Cell Signaling Tech. (# 9516) at a 1:100 dilution, with Alexa fluor 488 goat anti-rabbit secondary antibody (1:100 dilution) from Invitrogen (A11008). Nuclei were detected by incubating embryos with TO-PRO3 (ThermoFisher Scientific T3605) at a 1:300 dilution overnight with the secondary antibody. In all whole-mount immunolabeling assays, experimental embryos and the corresponding littermate controls were processed in the same tube throughout the procedure.

2.4. Confocal microscopy and image processing

After whole-mount ROS detection, cell death, or immuno-fluoresence, limbs were embedded in 1% low-melt agarose (Promega V2111) in a glass bottom dish (MatTek p35G-1.5–20–C), and covered in PBS. An LSM780 laser scanning confocal microscope (CarlZeiss) was used for image acquisition, assisted by the Optical Microscopy and Analysis Laboratory. Sum-projections were generated and stitched utilizing Fiji software (National Institutes of Health) (Preibisch et al., 2009).

2.5. Planar x-ray

Planar X-ray data were obtained through the Small Animal Imaging Program (SAIP) at the National Cancer Institute – Frederick. Adult mice were euthanized per use of laboratory animals guidelines, limbs were removed and immobilized using medical tape and paper. X-ray computed images were generated using a NanoSPECT/CT (Mediso Medical Imaging Systems, Budapest, Hungry).

2.6. Measurements and statistics

For all analyses at least three specimens were examined. In Fig. 2 panel J, measurements were made using the ruler tool in Adobe Photoshop CS4 (Version 11), error bars were calculated using the standard error of the mean, and significance was determined using a two-tailed *t*-test.

3. Results

To investigate the role of BMP signaling in interdigital PCD, we generated mutants with Osr1Cre-mediated recombination of each of the three ligand genes, *Bmp2, Bmp4,* or *Bmp7* (see Table 1; Materials and Methods). Osr1Cre is active within the interdigital mesenchyme of the developing limb bud (Grieshammer et al., 2008). Throughout this report, in all ID-specific BMP pathway mutants, we limit our analysis to hindlimb data because the greater separation between digits 1 and 2 that occurs in normal controls allows for clearer analysis of the ID tissue (ID 1) between these digits. However, the phenotypes we describe are true for both forelimb and hindlimb. To evaluate the efficiency of *Bmp* inactivation we used RNA *in situ* hybridization with a probe specific to the floxed region of each ligand gene at embryonic day (E) 13.5, around the time of PCD initiation in the hindlimbs. At this stage, normal *Bmp2* expression is evident in the borders between the ID and digits (ID/digit border) (Fig. 1A). Many of these domains are absent in Osr1Cre; $Bmp2^{flox/flox}$ mutants, with the greatest reduction in expression in ID 2 and 3 (Fig. 1B, black arrows), where expression remains only in the sub-AER region. In ID 1 and 4 a reduction also occurs, but less so than in ID 2 and 3, because of remaining *Bmp2* expression along the ID/digit border regions (Fig. 1B, yellow arrows). At this stage, normal ID *Bmp4* expression is most apparent in the sub-AER mesenchyme with lighter expression in the ID/digit borders (Fig. 1C). This border expression is reduced in Osr1Cre; $Bmp4^{flox/null}$ mutants (Fig. 1D). Of the three *Bmps,* normal ID *Bmp7* expression is most obvious (Fig. 1E). In Osr1Cre; $Bmp7^{flox/flox}$ mutants, *Bmp7* expression is mostly absent in the interdigital mesenchyme (Fig. 1F, black arrows) but, like Osr1Cre; $Bmp2^{flox/flox}$ mutants, some expression remains in sub-AER regions and along the ID/digit border in ID 1 and 4 (Fig. 1F, yellow arrows).

To monitor effects on BMP signaling, we assayed for *Msx2* expression, a well characterized BMP target expressed in the ID (Brugger et al., 2004). Although there were no changes in *Msx2* expression in *Bmp2* or *Bmp4* mutants (Fig. 1G–J), Osr1Cre; $Bmp7^{flox/flox}$ mutants showed a noticeable reduction within ID 2 and 3 (Fig. 1K, L). Finally, we examined adult hindlimbs of all mutants at about postnatal day (P) 22. Paralleling Msx2 expression, ID tissue regression was normal in *Bmp2* and *Bmp4* mutants (Fig. 1M–P), however, Osr1Cre; $Bmp7^{flox/flox}$ hindlimbs had syndactyly in ID 2 and 3 (Fig. 1Q, R). Therefore, we conclude that Osr1Cre-specific inactivations of *Bmp2* or *Bmp4* have negligible effects on BMP signaling and interdigital cell death whereas such an inactivation of *Bmp7* leads to a reduction of BMP signaling in ID 2 and 3 and results in syndactyly in these regions. It is likely that the lack of reduction in BMP signaling in Osr1Cre; $Bmp7^{flox/flox}$ ID 1 and 4 is due to the remaining *Bmp7* expression in these tissues (Fig. 1F, yellow arrows).

Even though our analysis indicates that, within the domain of Osr1Cre expression, BMP2 and BMP4 are not individually required for interdigital PCD, these ligands may play redundant roles in this process. To test this, we inactivated pairs of *Bmp* genes simultaneously with Osr1Cre (see Table 1). Inactivation of *Bmp2* and *Bmp7* or *Bmp4* and *Bmp7* resulted in syndactyly within ID 2 and 3 that was comparable to what we observed in loss of *Bmp7* alone (Fig. 2A–D). Hence, these genotypes shed no light on possible redundant roles for *Bmp2* and *Bmp4* in this process. However, the pairwise Osr1Cre-mediated inactivation of *Bmp2* and *Bmp4* results in syndactyly within ID 2 and 3 with incomplete penetrance (5/9 animals), demonstrating redundant roles for both of these genes in ID cell death (Fig. 2E). To explore this insight further we examined limbs in which we inactivated one allele of *Bmp7,* which does not by itself cause syndactyly (Fig. 2F), to sensitize the limb and then further inactivated both alleles of either *Bmp2* or *Bmp4* (see Table 1). Whereas we observed no syndactyly in Osr1Cre; $Bmp4^{flox/flox}$; $Bmp7^{flox/wt}$, we did find webbing in ID 2 and 3 of Osr1Cre; $Bmp2^{flox/flox}$; $Bmp7^{flox/wt}$ hindlimbs with complete penetrance (Fig. 2F–H). Finally, we generated mutant hindlimbs where we inactivated all three *Bmp* genes simultaneously with Osr1Cre. The resulting syndactylous hindlimbs resembled all previous samples in that ID 2 and 3 were webbed, but the degree of syndactyly was greater than what we have previously observed in other genotypes (Fig. 2A, I, J). Together these data demonstrate that genetic redundancy exists between these three *Bmp* genes in regard to interdigital PCD. Also, within the domain of Osr1Cre activity, a hierarchy exists in which *Bmp7* has the greatest effect on PCD, *Bmp2* has a moderate role and, lastly, *Bmp4* has the least effect.

Given that *Bmp7* is required for normal interdigital PCD and *Bmp2* and *Bmp4* play redundant roles in this process, we decided to further analyze “triple” mutants (Osr1Cre; $Bmp2^{flox/flox}$; $Bmp4^{flox/flox}$; $Bmp7^{flox/flox}$). We considered that with six floxed alleles, recombination might be less efficient than that of the individual *Bmp* gene inactivations. Thus, we again examined expression of *Bmp2, Bmp4,* and *Bmp7* in the triple mutants using the same probes, internal to the loxP sites, used in Fig. 1A–F and observed changes in expression comparable to that found in individual *Bmp* inactivations (Supplemental Fig. S1). These data indicate that Osr1Cre-mediated inactivation of all three *Bmp* ligand genes is as efficient as that seen in single inactivations. We also examined *Bmp2, Bmp4,* and *Bmp7* expression in the AER of triple mutants and found no difference between mutants and

controls; in both sets, expression was downregulated above the ID and remained overlying the digits (data not shown).

Next, we examined *Msx2* expression to monitor BMP signaling in the triple mutant and found a substantial decrease in expression in ID 2 and 3, while expression in ID 1 and 4 was unchanged from littermate controls (Fig. 3A and B). We surmise that the lack of a phenotype in ID 1 and 4 is due to the remaining *Bmp* ligand gene expression in these regions (Supplemental Fig. S1), as was the case in the single *Bmp* gene inactivations.

To determine whether syndactyly was due to perturbing interdigital PCD earlier in development, we examined E13.5 hindlimbs of triple mutant embryos stained with LysoTracker Red, a fluorescent marker that detects dying cells (Zucker et al., 1998). A significant reduction in LysoTracker Red was observed in ID 2 and 3 (Fig. 3C, D). We then assayed for the cleaved, and therefore activated, form of the main executioner of apoptosis, Caspase-3 and likewise found a notable reduction in signal in ID 2 and 3 of triple mutants (Fig. 3E, F).

We have previously shown that BMP signaling indirectly controls interdigital PCD by regulating the normal cessation of AER-specific expression of *Fgf8,* which encodes a cell survival activity for the ID (Pajni-Underwood et al., 2007). Therefore, even though we demonstrate a decrease in expression of interdigital *Msx2,* and hence BMP signals to this mesenchyme, it is possible that loss of these BMP ligand genes may affect *Fgf8* expression in the AER. However, we found that in triple mutants *Fgf8* expression was downregulated normally in the AER overlying the ID when compared to littermate controls (Fig. 3G and H), suggesting that AERFGF signaling is unaffected. We also investigated the activity of the RA signaling pathway, which produces another cell death signal in the limb bud ID (Hernandez-Martinez and Covarrubias, 2011). To monitor this pathway, we assayed for *Rarβ* expression, which encodes an RA receptor and is itself a target of RA signaling (de The et al., 1989; Zhao et al., 2009). *Rarβ* expression was unchanged in triple mutants (Fig. 3I, J).

Together, these data indicate that combined Osr1Cre mediated inactivation of *Bmp2, Bmp4,* and *Bmp7* is sufficient to dramatically downregulate BMP signaling in ID 2 and 3 and cause syndactyly. Loss of BMP signaling in these mutants apparently does not affect FGF or RA signaling, and therefore these BMP ligands appear to be direct cell death signals and effectors of apoptosis in the ID.

However, because these genes encode secreted ligands that can diffuse and possibly initiate BMP signaling in adjacent tissues, we cannot rule out that the observed decreases in PCD and syndactyly are indirect, acting through a signaling cascade other than FGF or RA. Therefore, to conclusively determine if BMPs directly trigger PCD during normal limb development we sought to abolish cell-autonomous BMP signaling *to* the interdigital mesenchyme. Thus, we used Osr1Cre to inactivate the gene encoding the BMP receptor BMPR1A specifically within the ID. Hindlimbs of adult Osr1Cre; $Bmpr1a^{flox/null}$ mutants displayed syndactyly in a different pattern than that observed in triple ligand mutants. The greatest degree of syndactyly occurred in ID 1, with webbing occurring all the way to the distal tip of digit 1 (Fig. 4A, B). Compared to ID 1, the severity of syndactyly decreases in

ID 2 and 3 and is minimal, although present, in ID 4 (Fig. 4A, B). Due to the severity of syndactyly in these mutants the more anterior digits appeared shorter. Therefore, to confirm that the limbs were otherwise normal and skeletal formation was unaffected we examined planar X-ray scans (Fig. 4C, D) and skeletal preparations (data not shown). Both of these assays established that Osr1Cre; *Bmpr1a*$^{flox/null}$ mutants have the correct number of skeletal elements of the appropriate length. Furthermore, because both the soft tissue and skeletal elements can be visualized in the X-ray images, it is evident that due to the severity of the soft tissue syndactyly, digits 1 through 3 cannot properly extend and remain bent, thus making them appear shorter (Fig. 4C, D).

To determine if PCD regulation was perturbed in Osr1Cre; *Bmpr1a*$^{flox/null}$ mutants we examined changes in cell death at E13.5. A significant reduction in LysoTracker Red is observed from ID 1 through 3, while in ID 4 fluorescent levels are slightly reduced in the proximal region (Fig. 4E, F). The most significant reduction in LysoTracker Red fluorescence is observed in ID 1. A higher resolution image clearly shows that almost all cell death is abolished in the proximal part of ID 1, while fluorescence remains in the sub-AER mesenchyme (Fig. 4E', F'). We also examined cleaved Caspase3 production and found a similar graded pattern, where the greatest reduction was present in anterior ID tissue and the least in posterior ID tissue (Fig. 4G, H). The gradient in phenotype severity prompted us to reexamine Osr1Cre activity, which had been previously described (Grieshammer et al., 2008). We found that Osr1Cre activated the Cre reporters *Rosa26*^{R26R} (Soriano, 1999) or *Rosa26*^{mTmG} (Muzumdar et al., 2007) in a graded manner, with earlier and greater Cre activity in anterior IDs (Supplemental Fig. S2 and data not shown). Thus the graded severity of syndactyly in Osr1Cre; *Bmpr1a*$^{flox/null}$ mutants appears to be a function of the timing of onset and extent of Cre activity in the different ID regions.

We then again determined if this genetic manipulation was affecting only interdigital BMP signaling or whether it was also causing changes in RA or FGF signaling in E13.5 embryos, when interdigital PCD is occurring. In this case we compared these mutants to our previously described Msx2Cre; *Bmpr1a*$^{flox/null}$ mutants, which are syndactylous because of dysregulated and prolonged AER-FGF activity (Pajni-Underwood et al., 2007). Again, using Msx2 as a readout of BMP signaling, we found a substantial decrease in expression in all IDs of Osr1Cre; *Bmpr1a*$^{flox/null}$ mutants, although this decrease was markedly less in the most posterior ID (Fig. 5A, B). In Msx2Cre; *Bmpr1a*$^{flox/null}$ forelimbs (these mutants have no hindlimbs (Pajni-Underwood et al., 2007)), ID-specific expression of *Msx2* was not reduced, as expected (Fig. 5C, D). *AER-Fgf8* expression was normally downregulated over the interdigital mesenchyme in Osr1Cre; *Bmpr1a*$^{flox/null}$ mutants (Fig. 5E, F) as was the AER-specific expression of *Bmp2*, *Bmp4* and *Bmp 7* (data not shown). As expected, *AER-Fgf8* expression was dysregulated in Msx2Cre; *Bmpr1a*$^{flox/null}$ mutants with some expression remaining over ID areas (Fig. 5G, H). Examination of *Rarβ* revealed that RA signaling was unchanged in Osr1Cre; *Bmpr1a*$^{flox/null}$ limbs (Fig. 5I, J). However, *Rarβ* was downregulated in Msx2Cre; *Bmpr1a*$^{flox/null}$ mutants (Fig. 5K, L) consistent with the idea that FGFs antagonize RA signaling (Hernandez-Martinez et al., 2009).

Elevated levels of reactive oxygen species (ROS) are present in the ID (Salas-Vidal et al., 1998) and manipulating their levels demonstrates that they are important signals in causing

PCD (Eshkar-Oren et al., 2015; Salas-Vidal et al., 1998; Schnabel et al., 2006). Recently, Zelzer and coworkers have shown that the vasculature plays an essential role in providing ROS signals within the ID (Eshkar-Oren et al., 2015). Therefore we examined both of these components in our two models of syndactyly. Staining for PECAM revealed no significant reduction in interdigital vasculature that could account for the observed phenotypes (Fig. 6A–D). However, in both syndactylous mutants, we observed a significant decrease of ROS production. In the case of Osr1Cre; *Bmpr1a*$^{flox/null}$ mutants a similar anterior to posterior gradient in severity was evident (Fig. 6E, F), as we had observed with LysoTracker Red staining (Fig. 4E, F) and cleaved Caspase-3 (Fig. 4G, H). In Msx2Cre; *Bmpr1a*$^{flox/null}$ mutants, ROS production was generally down in all IDs (Fig. 6G, H). Therefore, the two signaling events that are required for interdigital PCD, a BMP death signal and the withdrawal of FGF survival signals, converge on the production of ROS during this process.

4. Discussion

By inactivating *Bmpr1a* specifically in the limb bud ID, we demonstrate that BMPs act as direct triggers of apoptotic cell death in this tissue. By generating single ID-specific inactivations of *Bmp2, Bmp4,* and *Bmp7*, we demonstrate that only BMP7 is necessary for interdigital PCD. A comprehensive series where we inactivate these *Bmp* genes in different combinations reveals that BMP2 and BMP4 are both redundant players, with BMP2 playing the more significant role compared to BMP4. These insights are limited to the domain and window of Osr1Cre expression; it is conceivable that more extensive Cre activity may provide further insights into the relevant contributions of these *Bmp* genes.

Importantly, while loss of BMP signaling in the ID caused syndactyly, none of these genetic manipulations affected AER-FGF or RA signaling. Conversely, interdigital BMP signaling is not diminished in Msx2Cre; *Bmpr1a*$^{flox/null}$ limbs, which are syndactylous due to prolonged AER-FGF signals (Pajni-Underwood et al., 2007). We found that these sustained AER-FGF signals result in a reduction of RA signaling in the distal interdigital mesenchyme, corroborating the previously described antagonistic relationship between these two pathways (Hernandez-Martinez et al., 2009). The requirement of RA for interdigital PCD may be direct and/or indirect, through the regulation of FGF and BMP signals (Fig. 7). Mouse mutants lacking RA signaling components are syndactylous and apparently completely lack ID *Bmp7* expression (Dupe et al., 1999; Zhao et al., 2010), which we show here is the primary BMP ligand acting within the ID. Exogenously added RA induced *Bmp4* and *Bmp7* expression in chick (Rodriguez-Leon et al., 1999) and *Bmp7* expression in mouse (Hernandez-Martinez et al., 2009) limb cultures. Consistent with the notion that RA affects PCD through BMP regulation, PCD in RA treated chick limbs was prevented by the addition of the BMP antagonist, NOGGIN (Rodriguez-Leon et al., 1999). Alternatively, Covarrubias and coworkers performed similar experiments in mouse explanted limbs and found no inhibition of RA-induced PCD, suggesting RA may act directly (Hernandez-Martinez et al., 2009), possibly through the production of the reactive oxygen species that act during this process (Schnabel et al., 2006). Our observation that RA signaling is intact in mutants with ID-specific loss of BMP signaling components (Figs. 3 and 5) but does not prevent the resulting syndactyly suggests that RA's cell death role in PCD may be indirect through interdigital BMP regulation. Therefore, we propose that two events must occur for normal

interdigital PCD: a BMP death signal must be provided and an FGF survival signal must be withdrawn (Fig. 7).

Our work contradicts previous studies that suggested BMPs do not directly activate interdigital PCD in the mouse (Hernandez-Martinez and Covarrubias, 2011). One part of this argument is based on expression patterns: genes encoding components of the BMP pathway were found to not be expressed or expressed at very low levels within areas undergoing PCD (Salas-Vidal et al., 2001). However, the genetics presented here demonstrate that even the apparent very low levels of *Bmp4* expression contribute to interdigital PCD.

Another set of data arguing against a direct BMP role is in explant experiments where inhibition of SMAD activity, a downstream component of the BMP pathway, with dorsomorphin, did not affect cell death (Hernandez-Martinez et al., 2009). Consistent with this observation we detect no discernable change in nuclear phospho-SMAD 1, 5 staining in proximal ID regions where PCD is reduced in Osr1Cre; $Bmpr1a^{flox/null}$ mutants (Supplemental Fig. S3). It is possible that there are changes in phospho-SMAD 1, 5 levels that immunostaining cannot detect. However, no syndactyly occurs when we block SMAD activity by inactivating *Smad4*, encoding the obligate co-Smad, with Osr1Cre (Supplemental Fig. S3). Thus we suggest that interdigital BMP death signals trigger a non-Smad-dependent pathway (Mu et al., 2012); future effort will work on exploring this idea. This is in contrast to BMP signaling in the AER, where BMP signals regulate the withdrawal of AER-FGF signals through a SMAD-dependent pathway (Benazet and Zeller, 2013; Choi et al., 2012; Maatouk et al., 2009; Pajni-Underwood et al., 2007; Wong et al., 2012). Lastly, it has been observed that NOGGIN-soaked beads have no effect on either RA-induced or normal interdigital PCD in the mouse, whereas it does affect PCD in the chick (Hernandez-Martinez et al., 2009). Perhaps these mouse experiments were performed at time points where the limb was refractive to NOGGIN, or the *in vitro* explant conditions resulted in loss of NOGGIN responsiveness. The *in vivo* experiments described in this report avoid these potential issues.

The observed gradient In the phenotype in Osr1Cre; $Bmpr1a^{flox/null}$ mutants, where ID 1 through 3 is most affected, is clearly a function of the timing and extent of Osr1Cre activity. But within the *Bmp* ligand mutants, a reduction in BMP signaling and ensuing syndactyly occurs only in ID 2 and 3. In these mutants, *Bmp* genes are intact in the AER, a source of BMP ligand activity that signals to the underlying mesenchyme (Choi et al., 2012; Maatouk et al., 2009). Additionally, domains of *Bmp* gene expression remain in ID 1 and 4, providing a non-cell autonomous activity that can provide a cell death signal to the entire interdigital mesenchyme. Finally, the involvement of another ligand, such as BMP5, could be acting in our *Bmp* ligand mutants (Zuzarte-Luis et al., 2004).

We have also analyzed our mutants for other aspects of limb development where BMP signaling is speculated to play a role. We had previously speculated that the ID is the source of BMPs that signal through BMPR1A in the AER to downregulate *Fgf4* and *Fgf8* (Pajni-Underwood et al., 2007), which was supported by the observation that when *Bmp2* and *Bmp4* are simultaneously inactivated in the early limb bud mesenchyme, AER-*Fgf8* is elevated and syndactyly ensues (Bandyopadhyay et al., 2006). However, the later

inactivations in the *Bmp* ligand mutants described here do not support this idea, since specific loss of ID BMP ligands does not affect AER-*Fgf8* expression. Also, inactivation of *Bmp2* and *Bmp4* within the AER caused AER-*Fgf8* upregulation, demonstrating that the AER is a source of BMPs signaling to itself (Choi et al., 2012; Maatouk et al., 2009). Another BMP role we considered was that proposed by Dahn and Fallon, who argued that ID BMPs may pattern the anterior/posterior identity of the adjacent digit (Dahn and Fallon, 2000). However, skeletal preparations of triple ligand mutants revealed normal digit formation (data now shown). Of course, this does not disprove this idea, because another BMP ligand, such as BMP5, may be important (Suzuki, 2013) or an earlier or more extensive interdigital Cre activity (Huang and Mackem, 2015) may be needed to reveal this function.

Eshkar-Oren et al. have recently shown that the interdigital vasculature regulates ROS production that is required for PCD. They suggest that the vasculature-ROS pathway might be a second layer, in addition to the BMP and FGF molecular signals controlling interdigital PCD, and thus provides a “double safety mechanism” to ensure PCD is limited to the ID (Eshkar-Oren et al., 2015). Consistent with this idea, we find that neither BMP death signals nor the loss of AER-FGF survival signals affect interdigital vascular development. However, we found that both signaling pathways converged on ROS production, demonstrating integration of these pathways and signals. Furthermore, Eshkar-Oren et al. found that a reduction in PCD due to genetically decreasing vascular density correlates with a decrease in interdigital BMP signaling and persistent AER-*Fgf8* expression (Eshkar-Oren et al., 2015). Therefore we suggest that proper expression of key *Bmp* and *Fgf* signaling genes may require a normal vasculature and that ROS production is downstream of the effects of these signaling cascades (Fig. 7).

BMP signaling has been implicated in inducing apoptosis in other aspects of embryogenesis including: cavitation in the preimplantation epiblast (Coucouvanis and Martin, 1999), tail development (Goldman et al., 2000), within enamel knot cells of the developing tooth (Jernvall et al., 1998), rhombencephalic neural crest (Graham et al., 1994) formation of the external genitalia (Suzuki et al., 2003) and nephrogenesis (Michos et al., 2004). It is not clear to what extent FGF survival signals are also important in these systems. For example, elevated BMP signals due to inactivation of the gene encoding the BMP antagonist, GREMLIN, causes excessive death in the E11.5 metanephric mesenchyme (Michos et al., 2004). It is possible that these BMP signals are causing a loss of *Fgf9* and *Fgf20*, which are required for survival of these cells at this stage of development (Barak et al., 2012). In another example, Yamada and coworkers have suggested that a decrease in apoptosis that occurs in the distal urethral epithelium due to *Bmpr1a* inactivation may be due to a lack of BMP death signals and/or due to augmentation of *Fgf8* expression, encoding a survival activity (Suzuki et al., 2003). Genetic manipulation that affects one set of signals, but not the other, as we have done here, can tease apart the respective requirements of these pathways.

Lastly, it is interesting to note that developing bat wings, compared to mouse limbs, have a modification of both FGF and BMP signaling with interdigital expression domains of both *Fgf8* and *Gremlin* to inhibit PCD (Weatherbee et al., 2006). In the webbed ID regions of duck hindlimbs, a *Gremlin* expression domain, that is absent in chicks, has been

characterized (Merino et al., 1999). To our knowledge, no one has examined changes in FGF signaling that might affect the webbing that occurs in duck feet. These observations suggest that BMP and FGF signals are modulated in different species for the evolutionary acquisition of webbed limbs.

Supplementary Material

Refer to Web version on PubMed Central for supplementary material.

Acknowledgments

We thank Cindy Elder and Erika Truffer for excellent technical assistance. We are grateful to Stephen Lockett (Optical Microscopy and Analysis Laboratory) for assistance with confocal microscopy, Joseph Kalen and the Small Animal Imaging Program for assistance with planar X-ray acquisition, and to Elazar Zelzer and Sharon Krief for technical advice and helpful discussion. Thanks to Naiche Adler, Alan Perantoni, and Jianjian Zhu for insightful comments on the manuscript. We thank Chuxia Deng for the *Smad4*^{flox} mice and Gregg Duester for the *Rarβ* plasmid. We greatly appreciate Chen-Ming Fan, Susan Mackem, and Yingzi Yang for helpful discussion. This work was supported by the Center for Cancer Research of the Intramural Research Program of the National Institutes of Health through the National Cancer Institute.

References

Anderson MJ, Naiche LA, Wilson CP, Elder C, Swing DA, Lewandoski M, 2013 TCreERT2, a transgenic mouse line for temporal control of Cre-mediated recombination in lineages emerging from the primitive streak or tail bud. PLoS One 8, e62479.

Bandyopadhyay A, Tsuji K, Cox K, Harfe BD, Rosen V, Tabin CJ, 2006 Genetic analysis of the roles of BMP2, BMP4, and BMP7 in limb patterning and skeletogenesis. PLoS Genet. 2, e216. [PubMed: 17194222]

Barak H, Huh SH, Chen S, Jeanpierre C, Martinovic J, Parisot M, Bole-Feysot C, Nitschke P, Salomon R, Antignac C, Ornitz DM, Kopan R, 2012 FGF9 and FGF20 maintain the stemness of nephron progenitors in mice and man. Dev. Cell 22, 1191–1207. [PubMed: 22698282]

Benazet JD, Zeller R, 2013 Dual requirement of ectodermal Smad4 during AER formation and termination of feedback signaling in mouse limb buds. Genesis 51, 660–666. [PubMed: 23818325]

Braunger BM, Demmer C, Tamm ER, 2014 Programmed cell death during retinal development of the mouse eye. Adv. Exp. Med. Biol 801, 9–13. [PubMed: 24664675]

Brugger SM, Merrill AE, Torres-Vazquez J, Wu N, Ting MC, Cho JY, Dobias SL, Yi SE, Lyons K, Bell JR, Arora K, Warrior R, Maxson R, 2004 A phylogenetically conserved cis-regulatory module in the Msx2 promoter is sufficient for BMP-dependent transcription in murine and Drosophila embryos. Development 131, 5153–5165. [PubMed: 15459107]

Chang W, Lin Z, Kulessa H, Hebert J, Hogan BL, Wu DK, 2008 Bmp4 is essential for the formation of the vestibular apparatus that detects angular head movements. PLoS Genet. 4, e1000050.

Choi KS, Lee C, Maatouk DM, Harfe BD, 2012 Bmp2, Bmp4 and Bmp7 are co-required in the mouse AER for normal digit patterning but not limb outgrowth. PloS One 7, e37826.

Conradt B, 2009 Genetic control of programmed cell death during animal development. Ann. Rev. Genet 43, 493–523. [PubMed: 19886811]

Coucouvanis E, Martin GR, 1999 BMP signaling plays a role in visceral endoderm differentiation and cavitation in the early mouse embryo. Development 126, 535–546. [PubMed: 9876182]

Dahn RD, Fallon JF, 2000 Interdigital regulation of digit identity and homeotic transformation by modulated BMP signaling. Science 289, 438–441. [PubMed: 10903202]

de The H, Marchio A, Tiollais P, Dejean A, 1989 Differential expression and ligand regulation of the retinoic acid receptor alpha and beta genes. EMBO J. 8, 429–433. [PubMed: 2542014]

Dupe V, Ghyselinck NB, Thomazy V, Nagy L, Davies PJ, Chambon P, Mark M, 1999 Essential roles of retinoic acid signaling in interdigital apoptosis and control of BMP-7 expression in mouse autopods. Dev. Biol 208, 30–43. [PubMed: 10075839]

Dyche WJ, 1979 A comparative study of the differentiation and involution of the Mullerian duct and Wolffian duct in the male and female fetal mouse. J. Morphol 162, 175–209. [PubMed: 537099]

Elliott J, Cayouette M, Gravel C, 2006 The CNTF/LIF signaling pathway regulates developmental programmed cell death and differentiation of rod precursor cells in the mouse retina in vivo. Dev. Biol 300, 583–598. [PubMed: 17054938]

Eshkar-Oren I, Krief S, Ferrara N, Elliott AM, Zelzer E, 2015 Vascular patterning regulates interdigital cell death by a ROS-mediated mechanism. Development 142, 672–680. [PubMed: 25617432]

Ghyselinck NB, Dupe V, Dierich A, Messaddeq N, Garnier JM, Rochette-Egly C, Chambon P, Mark M, 1997 Role of the retinoic acid receptor beta (RAR-beta) during mouse development. Int. J. Dev. Biol 41, 425–447. [PubMed: 9240560]

Goldman DC, Martin GR, Tam PP, 2000 Fate and function of the ventral ectodermal ridge during mouse tail development. Development 127, 2113–2123. [PubMed: 10769235]

Graham A, Francis-West P, Brickell P, Lumsden A, 1994 The signalling molecule BMP4 mediates apoptosis in the rhombencephalic neural crest. Nature 372, 684–686. [PubMed: 7990961]

Grieshammer U, Agarwal P, Martin GR, 2008 A Cre transgene active in developing endodermal organs, heart, limb, and extra-ocular muscle. Genesis 46, 69–73. [PubMed: 18257103]

Grieshammer U, Cebrian C, Ilagan R, Meyers E, Herzlinger D, Martin GR, 2005 FGF8 is required for cell survival at distinct stages of nephrogenesis and for regulation of gene expression in nascent nephrons. Development 132, 3847–3857. [PubMed: 16049112]

Guha U, Gomes WA, Kobayashi T, Pestell RG, Kessler JA, 2002 In vivo evidence that BMP signaling is necessary for apoptosis in the mouse limb. Dev. Biol 249, 108–120. [PubMed: 12217322]

Hassan M, Watari H, AbuAlmaaty A, Ohba Y, Sakuragi N, 2014 Apoptosis and molecular targeting therapy in cancer. BioMed Res. Int 2014, 150845.

Hernandez-Martinez R, Castro-Obregon S, Covarrubias L, 2009 Progressive interdigital cell death: regulation by the antagonistic interaction between fibroblast growth factor 8 and retinoic acid. Development 136, 3669–3678. [PubMed: 19820185]

Hernandez-Martinez R, Covarrubias L, 2011 Interdigital cell death function and regulation: new insights on an old programmed cell death model. Dev. Growth Differ 53, 245–258. [PubMed: 21338350]

Huang BL, Mackem S, 2015 Tamoxifen-dependent, inducible Bmp2CreER drives selective recombinase activity in early interdigital mesenchyme and digit collateral ligaments. PloS One 10, e0123325.

Jernvall J, Aberg T, Kettunen P, Keranen S, Thesleff I, 1998 The life history of an embryonic signaling center: BMP-4 induces p21 and is associated with apoptosis in the mouse tooth enamel knot. Development 125, 161–169. [PubMed: 9486790]

Joyner A, Wall N, 2008 Immunohistochemistry of whole-mount mouse embryos. CSH Protoc 2008, pdb prot4820.

Kastner P, Mark M, Ghyselinck N, Krezel W, Dupe V, Grondona JM, Chambon P, 1997 Genetic evidence that the retinoid signal is transduced by heterodimeric RXR/RAR functional units during mouse development. Development 124, 313–326. [PubMed: 9053308]

Lorda-Diez CI, Montero JA, Garcia-Porrero JA, Hurle JM, 2015 Interdigital tissue regression in the developing limb of vertebrates. Int. J. Dev. Biol 59, 55–62. [PubMed: 26374526]

Lossi L, Gambino G, 2008 Apoptosis of the cerebellar neurons. Histol. Histopathol 23, 367–380. [PubMed: 18072093]

Lu P, Minowada G, Martin GR, 2006 Increasing Fgf4 expression in the mouse limb bud causes polysyndactyly and rescues the skeletal defects that result from loss of Fgf8 function. Development 133, 33–42. [PubMed: 16308330]

Lussier M, Canoun C, Ma C, Sank A, Shuler C, 1993 Interdigital soft tissue separation induced by retinoic acid in mouse limbs cultured in vitro. Int. J. Dev. Biol 37, 555–564. [PubMed: 8180000]

Ma L, Martin JF, 2005 Generation of a Bmp2 conditional null allele. Genesis 42, 203–206. [PubMed: 15986484]

Maatouk DM, Choi KS, Bouldin CM, Harfe BD, 2009 In the limb AER Bmp2 and Bmp4 are required for dorsal-ventral patterning and interdigital cell death but not limb outgrowth. Dev. Biol 327, 516–523. [PubMed: 19210962]

Macias D, Ganan Y, Ros MA, Hurle JM, 1996 In vivo inhibition of programmed cell death by local administration of FGF-2 and FGF-4 in the interdigital areas of the embryonic chick leg bud. Anat. Embryol 193, 533–541. [PubMed: 8737809]

Macias D, Ganan Y, Sampath TK, Piedra ME, Ros MA, Hurle JM, 1997 Role of BMP-2 and OP-1 (BMP-7) in programmed cell death and skeletogenesis during chick limb development. Development 124, 1109–1117. [PubMed: 9102298]

Merino R, Rodriguez-Leon J, Macias D, Ganan Y, Economides AN, Hurle JM, 1999 The BMP antagonist Gremlin regulates outgrowth, chondrogenesis and programmed cell death in the developing limb. Development 126, 5515–5522. [PubMed: 10556075]

Michos O, Panman L, Vintersten K, Beier K, Zeller R, Zuniga A, 2004 Gremlin-mediated BMP antagonism induces the epithelial-mesenchymal feedback signaling controlling metanephric kidney and limb organogenesis. Development 131, 3401–3410. [PubMed: 15201225]

Mishina Y, Hanks MC, Miura S, Tallquist MD, Behringer RR, 2002 Generation of Bmpr/Alk3 conditional knockout mice. Genesis 32, 69–72. [PubMed: 11857780]

Montero JA, Hurle JM, 2010 Sculpturing digit shape by cell death. Apoptosis: Int. J. Program. Cell Death 15, 365–375.

Mu Y, Gudey SK, Landstrom M, 2012 Non-Smad signaling pathways. Cell Tissue Res. 347, 11–20. [PubMed: 21701805]

Muzumdar MD, Tasic B, Miyamichi K, Li L, Luo L, 2007 A global double-fluorescent Cre reporter mouse. Genesis 45, 593–605. [PubMed: 17868096]

Naiche LA, Holder N, Lewandoski M, 2011 . FGF4 and FGF8 comprise the wave-front activity that controls somitogenesis. Proc. Natl. Acad. Sci. USA 108, 4018–4023. [PubMed: 21368122]

Ngo-Muller V, Muneoka K, 2000 Influence of FGF4 on digit morphogenesis during limb development in the mouse. Dev. Biol 219, 224–236. [PubMed: 10694418]

Pajni-Underwood S, Wilson CP, Elder C, Mishina Y, Lewandoski M, 2007 BMP signals control limb bud interdigital programmed cell death by regulating FGF signaling. Development 134, 2359–2368. [PubMed: 17537800]

Preibisch S, Saalfeld S, Tomancak P, 2009 Globally optimal stitching of tiled 3D microscopic image acquisitions. Bioinformatics 25, 1463–1465. [PubMed: 19346324]

Robert B, 2007 Bone morphogenetic protein signaling in limb outgrowth and patterning. Dev. Growth Differ 49, 455–468. [PubMed: 17661740]

Rodriguez-Leon J, Merino R, Macias D, Ganan Y, Santesteban E, Hurle JM, 1999 Retinoic acid regulates programmed cell death through BMP signalling. Nature Cell Biol. 1, 125–126. [PubMed: 10559885]

Salas-Vidal E, Lomeli H, Castro-Obregon S, Cuervo R, Escalante-Alcalde D, Covarrubias L, 1998 Reactive oxygen species participate in the control of mouse embryonic cell death. Exp. Cell Res 238, 136–147. [PubMed: 9457066]

Salas-Vidal E, Valencia C, Covarrubias L, 2001 Differential tissue growth and patterns of cell death in mouse limb autopod morphogenesis. Dev. Dyn 220, 295–306. [PubMed: 11307164]

Schnabel D, Salas-Vidal E, Narvaez V, Sanchez-Carbente Mdel R, Hernandez-Garcia D, Cuervo R, Covarrubias L, 2006 Expression and regulation of antioxidant enzymes in the developing limb support a function of ROS in interdigital cell death. Dev. Biol 291, 291–299. [PubMed: 16445905]

Soriano P, 1999 Generalized lacZ expression with the ROSA26 Cre reporter strain. Nature Gen. 21, 70–71.

Suzuki K, Bachiller D, Chen YP, Kamikawa M, Ogi H, Haraguchi R, Ogino Y, Minami Y, Mishina Y, Ahn K, Crenshaw EB 3rd, Yamada G, 2003 Regulation of outgrowth and apoptosis for the terminal appendage: external genitalia development by concerted actions of BMP signaling [corrected]. Development 130, 6209–6220. [PubMed: 14602679]

Suzuki T, 2013 How is digit identity determined during limb development? Dev. Growth Differ 55, 130–138. [PubMed: 23230964]

Takeuchi O, Fisher J, Suh H, Harada H, Malynn BA, Korsmeyer SJ, 2005 Essential role of BAX,BAK in B cell homeostasis and prevention of autoimmune disease. Proc. Natl. Acad. Sci. USA 102, 11272–11277. [PubMed: 16055554]

Teixeira J, Maheswaran S, Donahoe PK, 2001 Mullerian inhibiting substance: an instructive developmental hormone with diagnostic and possible therapeutic applications. Endocr. Rev 22, 657–674. [PubMed: 11588147]

Tower J, 2015 Programmed cell death in aging. Ageing Res. Rev 23, 90–100. [PubMed: 25862945]

Vermeulen K, Van Bockstaele DR, Berneman ZN, 2005 Apoptosis: mechanisms and relevance in cancer. Ann. Hematol 84, 627–639. [PubMed: 16041532]

Wang CK, Omi M, Ferrari D, Cheng HC, Lizarraga G, Chin HJ, Upholt WB, Dealy CN, Kosher RA, 2004 Function of BMPs in the apical ectoderm of the developing mouse limb. Dev. Biol 269, 109–122. [PubMed: 15081361]

Weatherbee SD, Behringer RR, Rasweiler J.Jt, Niswander LA, 2006 Interdigital webbing retention in bat wings illustrates genetic changes underlying amniote limb diversification. Proc. Natl. Acad. Sci. USA 103, 15103–15107. [PubMed: 17015842]

Wilkie AO, Patey SJ, Kan SH, van den Ouweland AM, Hamel BC, 2002 FGFs, their receptors, and human limb malformations: clinical and molecular correlations. Am. J. Med. Genet 112, 266–278. [PubMed: 12357470]

Wong YL, Behringer RR, Kwan KM, 2012 Smad1/Smad5 signaling in limb ectoderm functions redundantly and is required for interdigital programmed cell death. Dev. Biol 363, 247–257. [PubMed: 22240098]

Yokouchi Y, Sakiyama J, Kameda T, Iba H, Suzuki A, Ueno N, Kuroiwa A, 1996 BMP-2/−4 mediate programmed cell death in chicken limb buds. Development 122, 3725–3734. [PubMed: 9012494]

Young RW, 1984 Cell death during differentiation of the retina in the mouse. J. Comp. Neurol 229, 362–373. [PubMed: 6501608]

Zakeri Z, Penaloza C, Smith K, Ye Y, Lockshin RA, 2015 What cell death does in development. Int. J. Dev. Biol 59, 11–22. [PubMed: 26374521]

Zhao X, Brade T, Cunningham TJ, Duester G, 2010 Retinoic acid controls expression of tissue remodeling genes Hmgn1 and Fgf18 at the digit-interdigit junction. Dev. Dyn 239, 665–671. [PubMed: 20034106]

Zhao X, Sirbu IO, Mic FA, Molotkova N, Molotkov A, Kumar S, Duester G, 2009 Retinoic acid promotes limb induction through effects on body axis extension but is unnecessary for limb patterning. Curr. Biol 19, 1050–1057. [PubMed: 19464179]

Zou H, Niswander L, 1996 Requirement for BMP signaling in interdigital apoptosis and scale formation. Science 272, 738–741. [PubMed: 8614838]

Zouvelou V, Passa O, Segklia K, Tsalavos S, Valenzuela DM, Economides AN, Graf D, 2009 Generation and functional characterization of mice with a conditional BMP7 allele. Int. J. Dev. Biol 53, 597–603. [PubMed: 19247966]

Zucker RM, Hunter S, Rogers JM, 1998 Confocal laser scanning microscopy of apoptosis in organogenesis-stage mouse embryos. Cytometry 33, 348–354. [PubMed: 9822346]

Zuzarte-Luis V, Hurle JM, 2002 Programmed cell death in the developing limb. In. J. Dev. Biol 46, 871–876.

Zuzarte-Luis V, Hurle JM, 2005 Programmed cell death in the embryonic vertebrate limb. Semin. Cell Dev. Biol 16, 261–269. [PubMed: 15797836]

Zuzarte-Luis V, Montero JA, Rodriguez-Leon J, Merino R, Rodriguez-Rey JC, Hurle JM, 2004 A new role for BMP5 during limb development acting through the synergic activation of Smad and MAPK pathways. Dev. Biol 272, 39–52. [PubMed: 15242789]

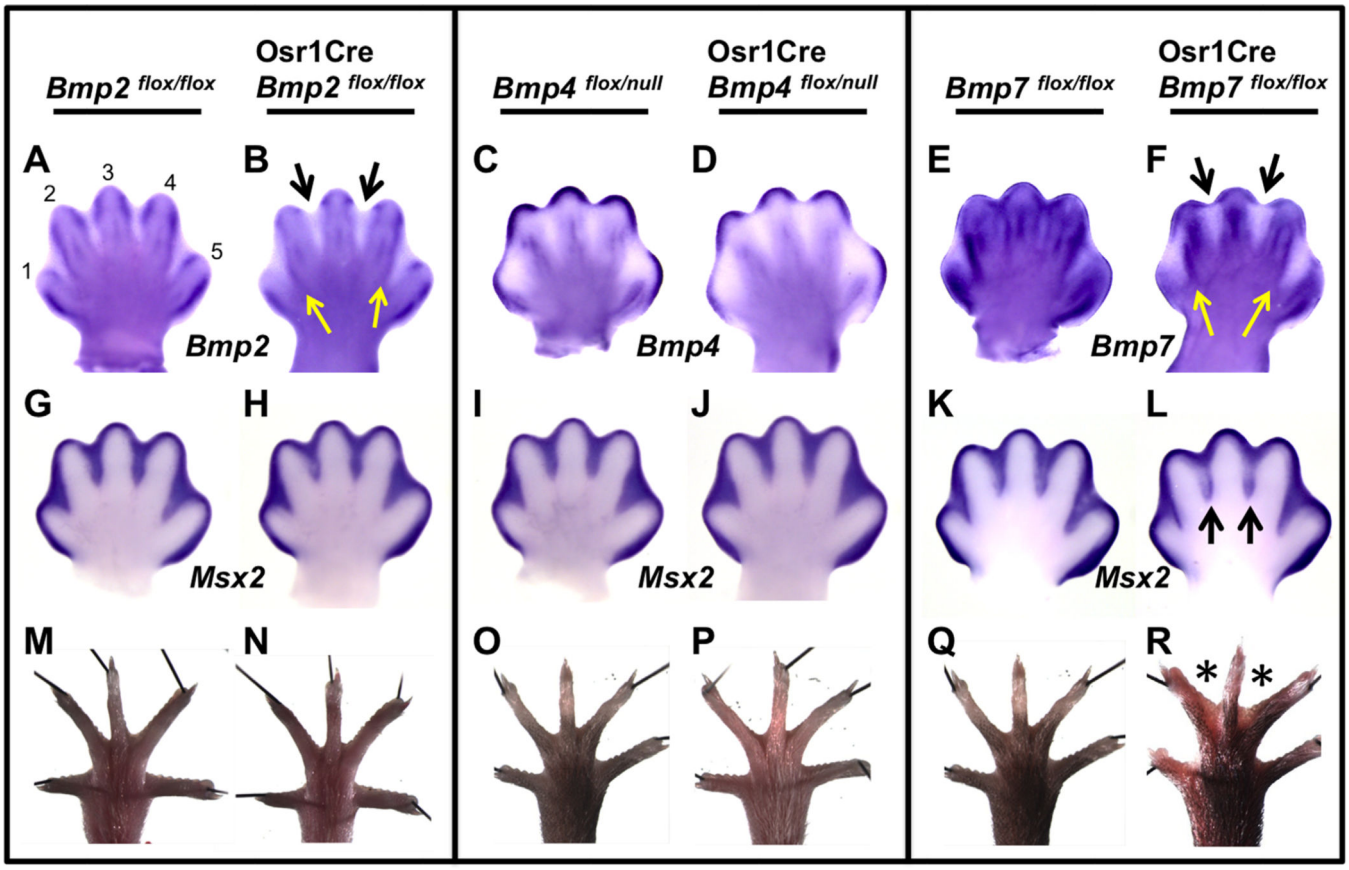

Fig. 1.

Limb ID-specific inactivation of *Bmp7* results in a decrease of BMP signaling and soft-tissue syndactyly. (A–L) Whole-mount *in situ* hybridization (WISH) assays were performed using the riboprobe indicated on E13.5 hindlimbs of embryos of the specified genotype. (A–F) The indicated riboprobe is complementary to the region of DNA deleted by Cre and therefore can only detect the mRNA derived from the unrecombined allele. In Osr1Cre; *Bmp2*$^{flox/flox}$ (B) and Osr1Cre; Bmp*7*$^{flox/flox}$ (F) mutants, expression is absent in ID 2 and 3 (black arrows) except for a small region in the sub-AER mesenchyme. In ID 1 and 4 of these mutants, expression is mostly absent except along the ID/ digit border (yellow arrows). (G–L) Msx2 expression. A downregulation was observed only in ID 2 and 3 of Osr1Cre; *Bmp7*$^{flox/flox}$ mutants (L, black arrows). (M–R) Adult hindlimbs; black lines are pins holding samples in place. Syndactyly (asterisks) is observed in hindlimbs of Osr1Cre; *Bmp7*$^{flox/flox}$ mutants (R) but not in other genotypes. All views are dorsal with anterior to the left. Numbers 1 through 5 denote corresponding digits.

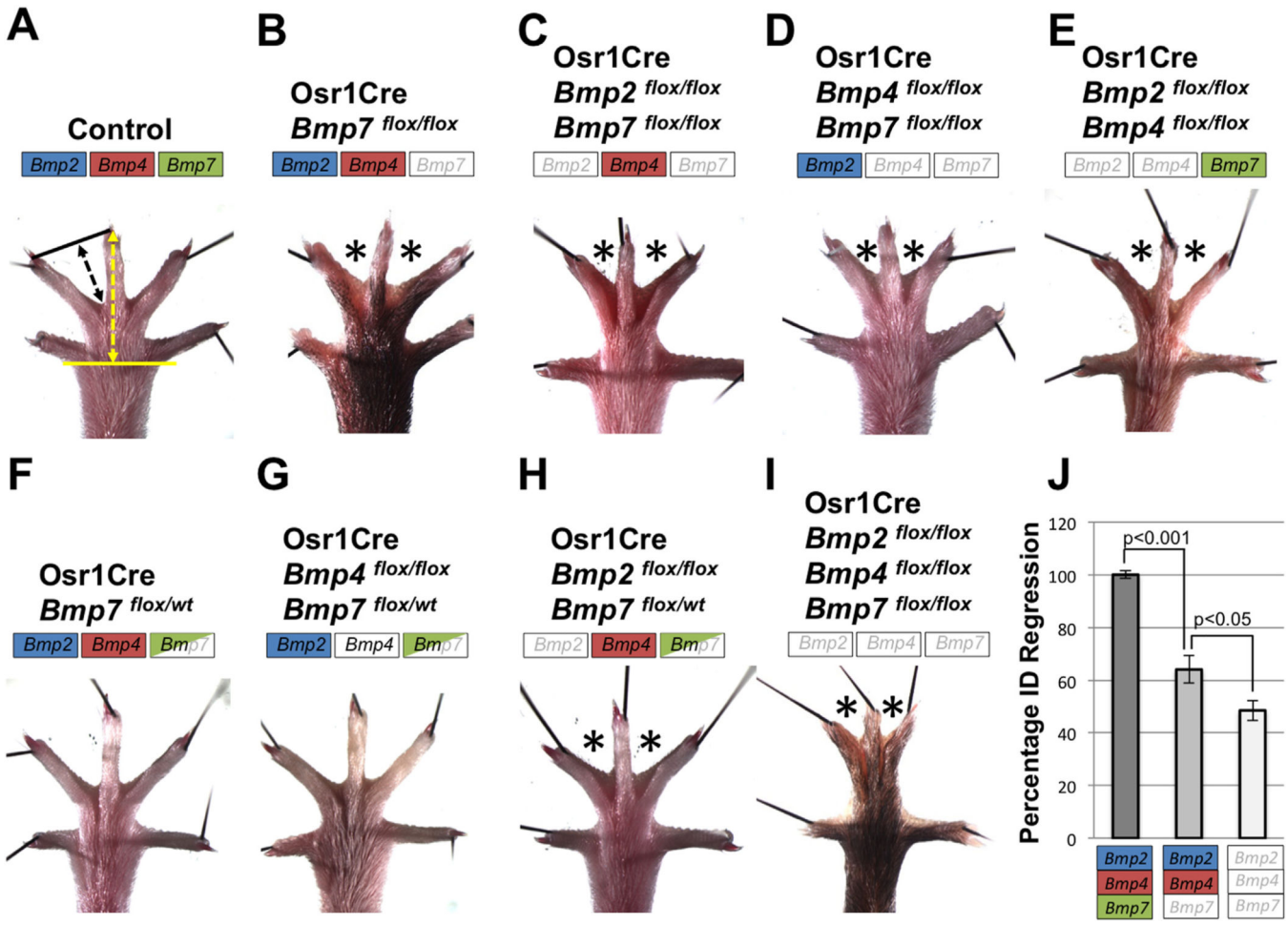

Fig. 2.

Bmp2, Bmp4, and *Bmp7* have redundant roles in ID tissue regression. (A-I) Adult hindlimbs of mice with the specified genotype were examined for syndactyly (asterisks). Color boxes indicate status of allele inactivation by Osr1Cre; a fully colored box indicates two wildtype alleles, a half-colored box indicates heterozygosity for a floxed allele and a white box indicates two floxed alleles. (J) Quantification of ID regression of the genotypes indicated was determined by measuring the length specified by the black arrow (A) and normalizing to the length specified by the yellow arrow (A). Error bars represent SEM and a two-tailed *t*-test was performed to determine significance. Complete penetrance of phenotype was observed in all cases, except for Osr1Cre; $Bmp2^{flox/flox}$; $Bmp4^{flox/flox}$ mutants (E) which occurred in 5/9 animals. All views are dorsal with anterior to the left.

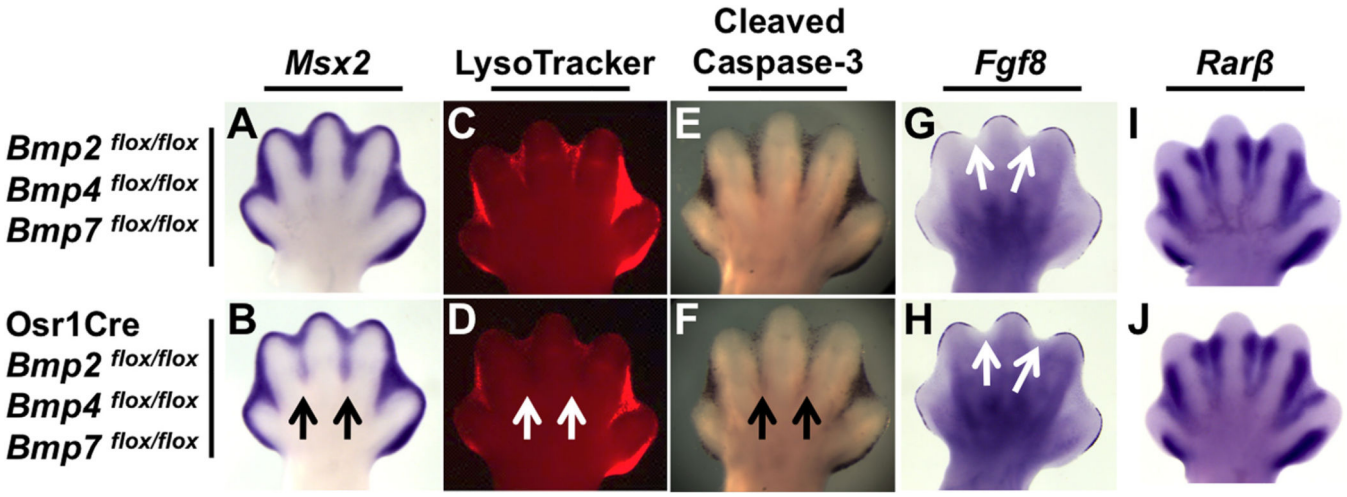

Fig. 3.

ID-specific *Bmp2, Bmp4,* and *Bmp7* inactivation results in a decrease in apoptotic cell death. (A-J) E13.5 hindlimbs of Osr1Cre; $Bmp2^{flox/flox}$; $Bmp4^{flox/flox}$; $Bmp7^{flox/flox}$ mutants (B, D, F, H, J) and littermate controls (A, C, E, G, I). (A, B) WISH assay for *Msx2* mRNA (black arrows indicate downregulation). (C, D) LysoTracker Red and (E, F) cleaved Caspase-3 immunostaining (white arrows, D, and black arrows, F, indicate reduced cell death in ID 2 and 3 of mutants). (G–J) WISH assays for *Fgf8* or *Rarβ*. Note, *Fgf8* is appropriately downregulated in the AER overlying the ID region (white arrows, G, H). All views are dorsal with anterior to the left.

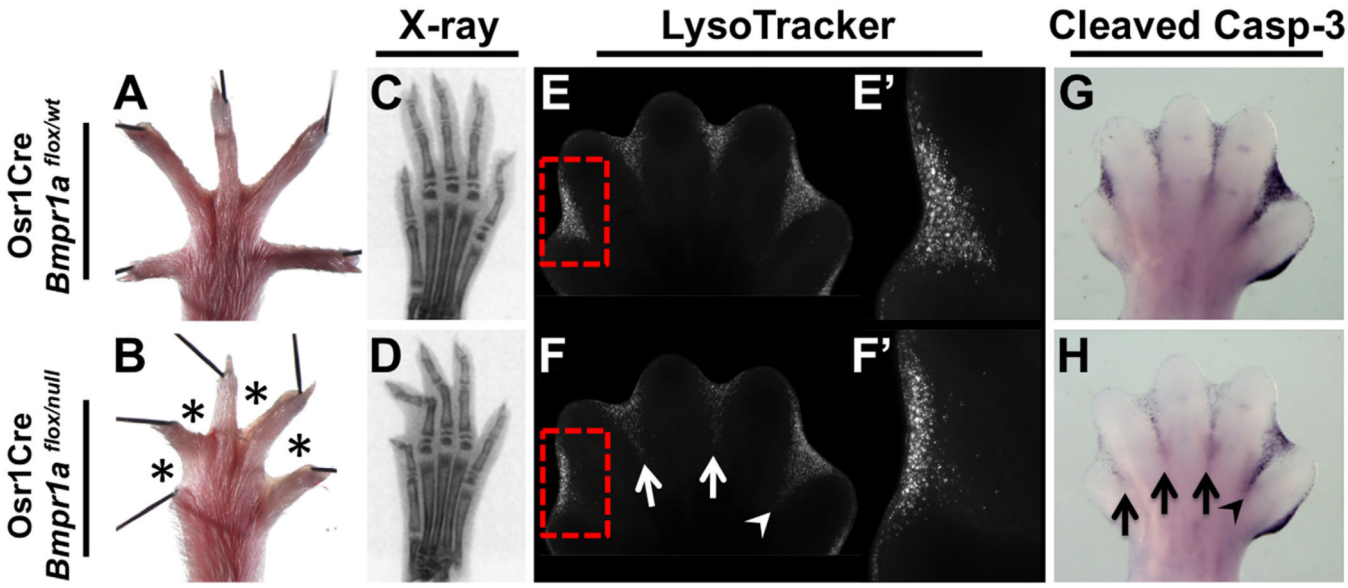

Fig. 4.

ID-specific *Bmpr1a* inactivation results in soft-tissue syndactyly and a decrease in apoptotic cell death. (A, B) Syndactyly (asterisks) is observed in adult hindlimbs of Osr1Cre; *Bmpr1a*$^{flox/null}$ mutants. (C, D) Planar X-ray scans, showing normal skeletal elements. (E, F) LysoTracker Red staining. The most significant change in mutants occurs in ID 1 (red box, E', F'), with more modest changes occurring in ID 2 and 3 (white arrows) and a minimal change in the proximal region of ID 4 (white arrowhead). (G, H) Cleaved Caspase-3 staining. The most significant change in mutants occurs in ID 1, 2 and 3 (black arrows) with a smaller change in ID 4 (black arrowhead). All views are dorsal with anterior to the left.

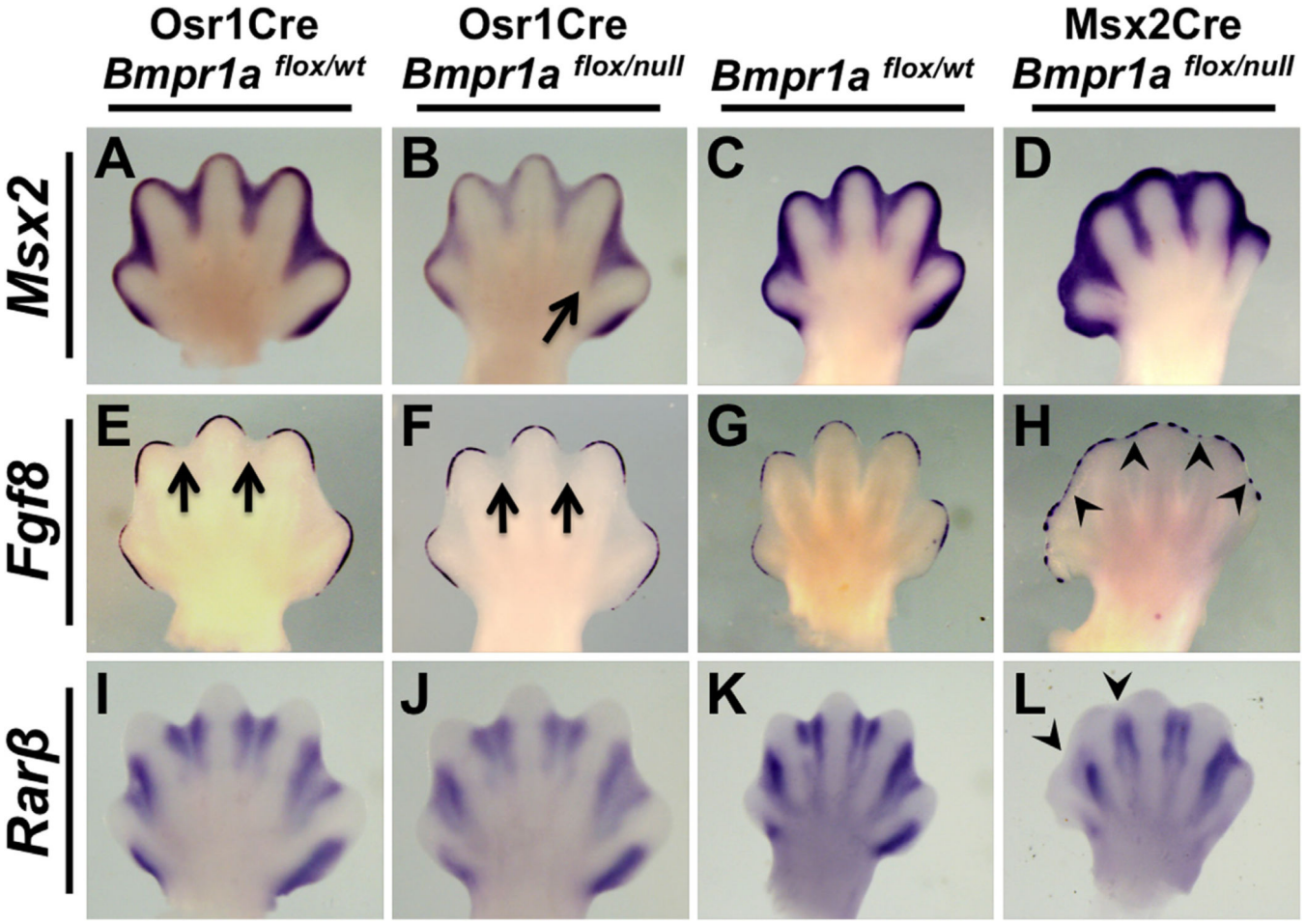

Fig. 5.

Analysis of the BMP, AER-FGF, and RA pathways in mutants with ID- or AER-specific inactivation of *Bmpr1a*. (A–L) WISH assays using the riboprobe indicated on E13.75 hindlimbs of Osr1Cre; *Bmpr1a*$^{flox/null}$ (B, F, J) or E13.25 forelimbs of Msx2Cre; *Bmpr1a*$^{flox/null}$ (D, H, L) and littermate controls (A, E, I, C, G, K). Arrow in B indicates a less severe downregulation of *Msx2* expression in ID 4 compared to other IDs. Arrows in E, F indicates normal downregulation of *Fgf8* above ID. Arrowheads in H indicate retention of AER-*Fgf8* expression overlying ID. Arrowheads in L indicate an absence of *Rarβ* expression in the distal areas of ID 1 and 2. All views are dorsal with anterior to the left.

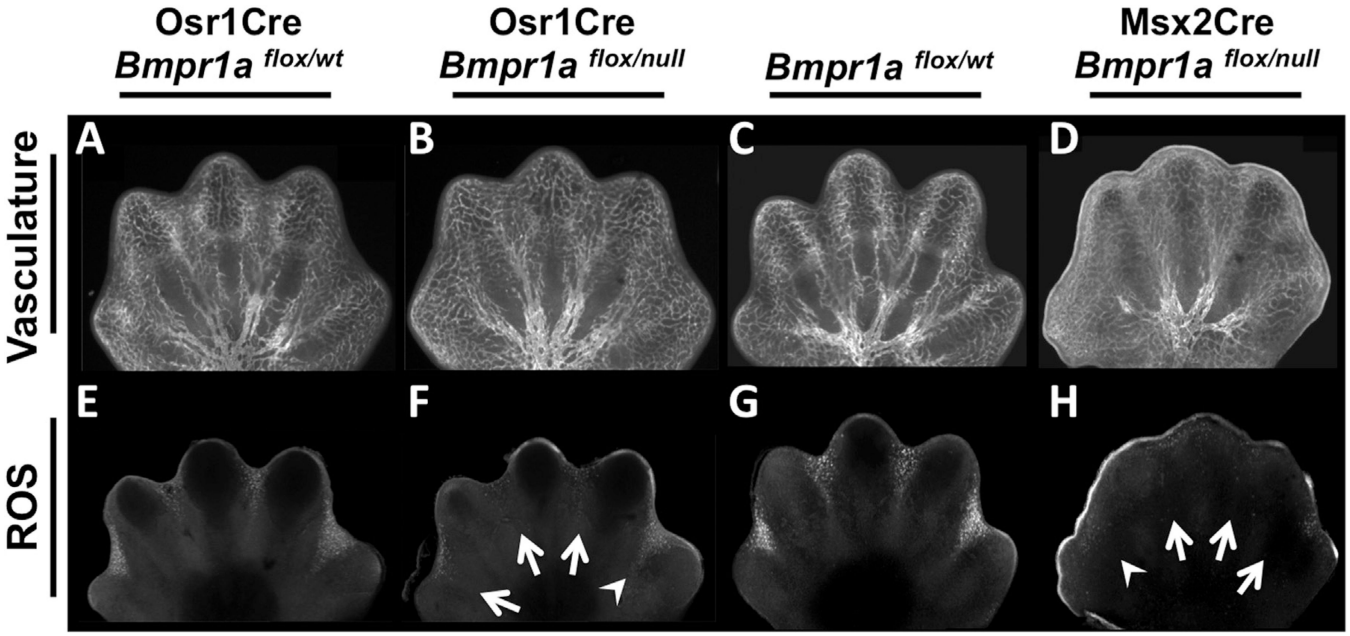

Fig. 6.

ID- or AER-specific *Bmpr1a* inactivation does not affect vascular patterning but results in a decrease of reactive oxygen species. (A–H) Confocal images of E13.75 hindlimbs of Osr1Cre; $Bmpr1a^{flox/null}$ (B, F) or E13.25 forelimbs of Msx2Cre; $Bmpr1a^{flox/null}$ (D, H) mutants and littermate controls (A, C, E, G). (A–D) PECAM whole-mount immunofluorescence to detect vascular patterning. (E–H) Dihydroethidium whole-mount staining to detect reactive oxygen species (ROS). Arrows indicate complete downregulation in ROS, arrowheads indicate a less severe decrease in ROS.

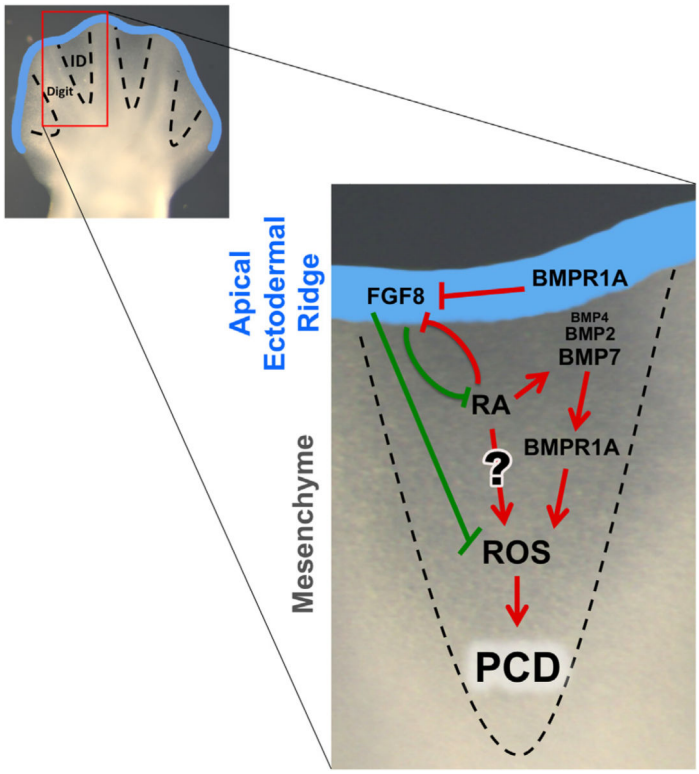

Fig. 7.

Two-event model for interdigital PCD. During normal development, both the withdrawal of an FGF cell survival factor from the AER and the activation of a BMP cell death factor in the interdigital mesenchyme are necessary for ID removal. BMP signaling through BMPR1A regulates interdigital PCD indirectly through AER-FGFs and directly within the ID. In addition, of the three BMP ligands ID, BMP7 is necessary for PCD during normal development, while BMP2 and, to a lesser extent, BMP4 act redundantly. RA can indirectly regulate ID PCD through FGF and BMP signaling, while its direct role is more uncertain (see text for details). Finally, interdigital BMP signals and the withdrawal of AER-FGF8 signals converge on ROS production, required for PCD. Red or green arrows denote that the end result is PCD or the inhibition of PCD, respectively.

Dev Biol. Author manuscript; available in PMC 2020 February 18.

Table 1

Genetic Crosses.

Experimental cross			**Experimental genotype (Freq)**		**Control genotype (Freq)**			
Bmp2 $^{flox/flox}$ [a]	X	Osr1Cre$^{Tg/0}$	Osr1Cre$^{Tg/0}$ [b]	(1/2)	*Bmp2* $^{flox/flox}$ [b]		(1/2)	
		Bmp2 $^{flox/flox}$	*Bmp2* $^{flox/flox}$					
Bmp4 $^{flox/flox}$ [a]	X	Osr1Cre$^{Tg/0}$	Osr1Cre$^{Tg/0}$ [b]	(1/4)	*Bmp4* $^{flox/null}$ [b]		(1/4)	
		Bmp4 $^{null/wt}$	*Bmp4* $^{flox/null}$					
Bmp7 $^{flox/flox}$ [a]	X	Osr1Cre$^{Tg/0}$	Osr1Cre$^{Tg/0}$ [b]	(1/2)	*Bmp7* $^{flox/flox}$ [b]		(1/2)	
		Bmp7 $^{flox/flox}$	*Bmp7* $^{flox/flox}$					
Bmp2 $^{flox/flox}$ [a]	X	Osr1Cre$^{Tg/0}$	Osr1Cre$^{Tg/0}$ [b]	(1/2)	*Bmp2* $^{flox/flox}$ [b]		(1/2)	
Bmp4 $^{flox/flox}$		*Bmp2* $^{flox/flox}$	*Bmp2* $^{flox/flox}$		*Bmp4* $^{flox/flox}$			
		Bmp4 $^{flox/flox}$	*Bmp4* $^{flox/flox}$					
Bmp2 $^{flox/flox}$ [a]	X	Osr1Cre$^{Tg/0}$	Osr1Cre$^{Tg/0}$ [b]	(1/2)	*Bmp2* $^{flox/flox}$ [b]		(1/2)	
Bmp7 $^{flox/flox}$		*Bmp2* $^{flox/flox}$	*Bmp2* $^{flox/flox}$		*Bmp7* $^{flox/flox}$			
		Bmp7 $^{flox/flox}$	*Bmp7* $^{flox/flox}$					
Bmp4 $^{flox/flox}$ [a]	X	Osr1Cre$^{Tg/0}$	Osr1Cre$^{Tg/0}$ [b]	(1/2)	*Bmp4* $^{flox/flox}$ [b]		(1/2)	
Bmp7 $^{flox/flox}$		*Bmp4* $^{flox/flox}$	*Bmp4* $^{flox/flox}$		*Bmp7* $^{flox/flox}$			
		Bmp7 $^{flox/flox}$	*Bmp7* $^{flox/flox}$					
Bmp2 $^{flox/flox}$	X	Osr1Cre$^{Tg/0}$	Osr1Cre$^{Tg/0}$	(1/16)	Osr1Cre$^{Tg/0}$	(1/16)	Osr1Cre$^{Tg/0}$	(1/8)
Bmp7 $^{flox/flox}$		*Bmp2* $^{flox/wt}$	*Bmp2* $^{flox/flox}$		*Bmp7* $^{flox/wt}$		*Bmp2* $^{flox/wt}$	
		Bmp7 $^{flox/wt}$	*Bmp7* $^{flox/wt}$				*Bmp7* $^{flox/wt}$	
Bmp2 $^{flox/flox}$ [a]	X	Osr1Cre$^{Tg/0}$	Osr1Cre$^{Tg/0}$	(1/2)	*Bmp2* $^{flox/flox}$ [b]		(1/2)	
Bmp4 $^{flox/flox}$		*Bmp2* $^{flox/flox}$	*Bmp2* $^{flox/flox}$		*Bmp4* $^{flox/flox}$			
Bmp7 flox/flox		*Bmp4* $^{flox/flox}$	*Bmp4* $^{flox/flox}$		*Bmp7* $^{flox/flox}$			
		Bmp7 $^{flox/flox}$	*Bmp7* $^{flox/flox}$					
Bmpr1a $^{flox/flox}$ [a]	X	Osr1Cre$^{Tg/Tg}$	Osr1Cre$^{Tg/0}$[b]	(1/2)	Osr1Cre$^{Tg/0}$[b]		(1/2)	

Experimental cross			Experimental genotype (Freq)		Control genotype (Freq)		
		Bmpr1a $^{null/wt}$	*Bmpr1a* $^{flox/null}$		*Bmpr1a* $^{null/wt}$		
Bmpr1a $^{flox/flox}$ [a]	X	Msx2Cre$^{Tg/0}$	Msx2Cre$^{Tg/0}$[b]	(1/2)[c]	*Bmpr1a* $^{flox/wt}$ [b]	(1/2)[c]	
		Bmpr1a $^{null/wt}$	*Bmpr1a* $^{flox/null}$				
Smad4 $^{flox/flox}$	X	Osr1Cre$^{Tg/Tg}$	Osr1Cre$^{Tg/0}$	(1/2)	Osr1Cre$^{Tg/0}$	(1/2)	
		Smad4 $^{null/wt}$	*Smad4* $^{flox/null}$		Smad4 $^{flox/wt}$		

[a] Parents also contain Rosa26 *mTmG/mTmG*.

[b] Progeny also contain Rosa26 *mTmG/wt*.

[c] *Bmpr1a* ^{null} and Msx2Cre are very closely linked (see Pajni-Underwood et al., 2007).